Water treatment intensification using a monophasic hybrid process coupling nanofiltration and ozone/hydrogen peroxide advanced oxidation

Sara Ouali, Pierre-Francois Biard, Patrick Loulergue, Rukun You, Noureddine Nasrallah, Rachida Maachi, Anthony Szymczyk

Water treatment intensification using a monophasic hybrid process coupling nanofiltration and ozone/hydrogen peroxide advanced oxidation

Sara Ouali[a,b], Pierre-François Biard[a*], Patrick Loulergue[a], Rukun You[a], Noureddine Nasrallah[b], Rachida Maachi[b], Anthony Szymczyk[a]

[a]Univ Rennes, Ecole Nationale Supérieure de Chimie de Rennes, CNRS, ISCR – UMR6226, F-35000 Rennes, France

[b]Faculté de Génie Mécanique et Génie des Procédés, Université des Sciences et de la Technologie Houari Boumediene, Algiers, Algeria

Abstract

This study assesses the feasibility of designing a hybrid ozonation / nanofiltration membrane process that can simultaneously oxidize and reject contaminants while exhibiting reduced membrane fouling. An innovative monophasic configuration, in which a pre-ozonated water was mixed at the membrane cell inlet to the water to be treated doped with H_2O_2 (at equimolar concentrations of H_2O_2 and O_3), was implemented, allowing to avoid an ozone-enriched gas flow in the membrane cell. Thus, two commercial polymer membranes, NP10 (polyethersulfone) and NF270 (polyamide), were assessed in a cross-flow configuration despite their low-ozone compatibility compared with ceramic membranes. Ozone removal yields greater than 90% were obtained whatever the studied water matrix. Fast ozone decomposition initiation reactions with H_2O_2 and with some moieties of the natural organic matter

* corresponding author: Pierre-Francois BIARD, pierre-francois.biard@ensc-rennes.fr, +33 2 23 23 81 49

were responsible for a low ozone lifetime in the liquid bulk, allowing to protect the membranes from ozone and radicals. Deethylatrazine (DEA) was used as a radical tracer, allowing to determine R_{ct} values with orders of magnitude of 10^{-6} and 10^{-7} in drinking water and a river water sample, respectively. The concentrations of two pharmaceuticals, carbamazepine and sulfamethoxazole, in the permeate and the retentate were lower than the detection limit in drinking water when the PES membrane was tested. During treatment of the river water sample, membrane fouling dropped by a factor two while there was no alteration of both the PES and PA membranes. Finally, thanks to synergistic effects induced by contaminant oxidation and rejection, dissolved organic content and DEA were both removed at around 70% when PA membrane, exhibiting a tighter microstructure than PES, was used.

Keywords

Nanofiltration; organic membrane; micropollutant; ozone; hydrogen peroxide; advanced oxidation process.

Graphical abstract

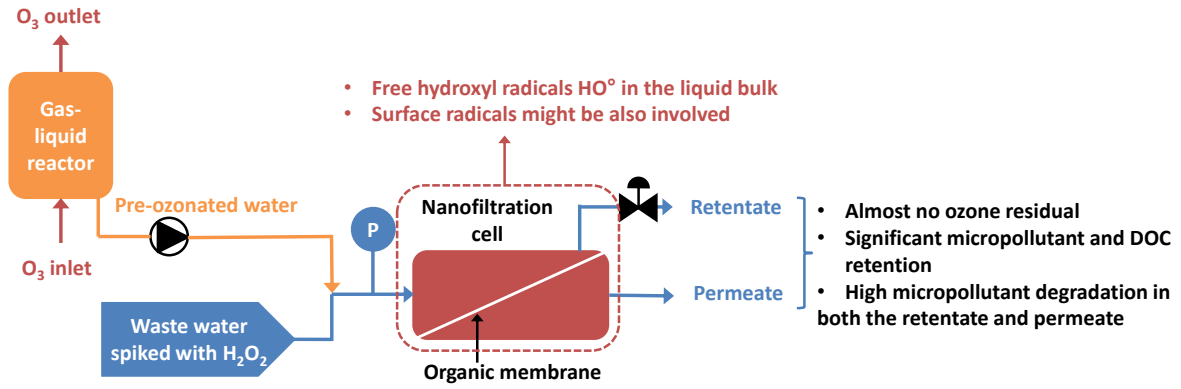

Nomenclature

$\{\int C_{Oz} dt\}$: ozone exposure (mol L^{-1} s)

$\{\int C_{HO^{\bullet}} dt\}$: hydroxyl radical exposure (mol L^{-1} s)

AOP: advanced oxidation process

C_i: concentration of any species i (in mol L^{-1} or ppm depending on the situation)

CBZ: carbamazepine

DEA: deethylatrazine

DOC: dissolved organic carbon

F_1: flow rate of the water to treat (L h^{-1})

F_2: flow rate of the pre-ozonated solution (L h^{-1})

F_F: total feedflow rate (L h^{-1})

FTIR: Fourier Transform InfraRed spectroscopy

HOMF: hybrid-ozone membrane filtration

HONF: hybrid-ozone membrane nanofiltration

$k_{MP,i}$: reaction rate constant between a MP and a species i (L mol^{-1} s^{-1})

LPRO: low pressure reverse osmosis

LOD: limit of detection (ppm)

LOQ: limit of quantification (ppm)

L_p: membrane permeability (L h^{-1} m^{-2} bar^{-1})

NF: nanofiltration

MWCO: molecular weight cut-off (Da)

NOM: natural organic matter

OTP: oxidation transformation product

PA: polyamide

PES: polyethersulfone

PVP: polyvinylpyrrolidone

R_{ct}: ratio of the hydroxyl radical exposure to the ozone exposure (dimensionless)

R_i: rejection rate of any species I (dimensionless)

RR: permeate recovery rate (dimensionless)

SMX: sulfamethoxazole

TMP: transmembrane pressure (bar)

Greek letters:

η_i : removal yields of any species i

$\Delta C_i/\Delta C_i'$: ratio of the amount of the species i consumed over the amount of the species i'

τ_{in}: hydraulic residence time between the mixing point and the membrane inlet (s)

τ_{ret}: hydraulic residence time in the retentate side (s)

Subscripts:

F: in the feed

HP: hydrogen peroxide

i : any species i

Oz: ozone

P: in the permeate

MP: micropollutant

R: in the retentate

1. Introduction

Micropollutants such as pesticides, personal care products, pharmaceuticals and their metabolites, etc.) are commonly present in natural water at concentrations lower than a few μg L^{-1} [1]. Micropollutants accumulation in natural waters is due to the fact that conventional treatments of drinking and waste waters and natural attenuation are not capable of removing micropollutants [2]. To address this new challenge, water management experts are paying a close attention to membrane filtration and advanced oxidation processes (AOP) as promising technologies in both drinking water and waste water treatment plants or for reuse purpose [3,4].

Organic solutes rejection using permselective membrane is governed by several mechanisms (size exclusion, hydrophobic/adsorptive interactions and electrostatic interactions) [5–7]. Only materials such as nanofiltration (NF) and dense low pressure reverse osmosis membranes (LPRO) are recommended to retain micropollutants (MP), which are characterized by low molecular weights [7–10]. Nonetheless, the shortcomings caused by some persistent membrane fouling issues and the handling of the rejected concentrate still create critical challenges in full-scale filtration systems [6].

AOPs are based on the generation of nonselective and highly reactive free radicals, such as the hydroxyl radicals $HO^{\bullet}$, to target refractory micropollutants [11]. Because of their high efficiency and level of maturity, ozonation and ozone-based AOPs are the most prominent oxidation processes in water treatment [4]. They are based on the ozone decomposition in water, which can be initiated by chemical species (HO^-, HO_2^- the hydroperoxyde anion which is the conjugated base of H_2O_2, heterogeneous catalysts, some natural organic matter moieties, etc.) or physical sources (ultrasound, UV) [12–16]. Nonetheless, ozone-based AOP applications are still limited, especially in drinking water production, by the fate of the oxidation transformation products (OTPs) [4,16]. Using the O_3/H_2O_2 process, addition of H_2O_2 allows to convert almost instantaneously dissolved ozone to hydroxyl radicals, decreasing drastically the ozone exposure (but not the total ozone dose), that is defined as the time integral of the ozone concentration [17]. It results in many cases in an improvement of MP removal efficiencies,

except for the case of MPs having a high reactivity with molecular ozone (characterized by bimolecular reaction rate constants roughly > 10^4 M^{-1} s^{-1}).

Thus, ozonation and membrane filtration coupling has been investigated in the literature to mitigate the drawbacks of each technology [6,18]. Several configurations have been proposed: (i) with a pre-ozonation, mainly to lower membrane fouling [19–22], (ii) with a post-ozonation to refine the permeate or treat the retentate [23,24] and (iii), as an hybrid process coupling both technologies in only one step [25–27]. Hybrid-ozone membrane filtration (HOMF) would allow to retain (membrane rejection) the OTPs and at the same time to mitigate the membrane fouling, allowing to improve the permeate quality and to pretreat the retentate [28]. It also offers the opportunity of combining two steps in only one toward process intensification [29]. Owing to the low chemical compatibility of many polymeric membranes with ozone [30], only ceramic membranes have been implemented. Moreover, up to now, HOMF has been applied only in gas-liquid systems, in which an ozone-enriched gas flow is introduced in the raw water at the membrane cell inlet [31].

In 2018, Biard *et al.* developed an AOP based on a monophasic configuration, in which a pre-ozonated makeup water was mixed in-line to a polluted water, advantageously spiked with H_2O_2 to enhance ozone decomposition, using a tubular reactor filled with static mixers. This configuration enables to enhance $HO^{\bullet}$ generation by taking advantage of the instantaneous ozone demand phase [32]. Besides, this configuration was particularly effective to control the ozone dose applied and allowed to generate the radicals directly in the liquid bulk whereas they are mainly generated at the gas-liquid interface using the gas-liquid configuration. Such a monophasic configuration applied to HOMF would allow to avoid an ozone-enriched gas-phase in contact with the membrane, enabling to consider cheaper organic membranes instead of ceramic ones.

Thus, the purpose of this study was to evaluate the potential of an innovative hybrid ozone membrane nanofiltration (HONF) in a monophasic configuration, using ozone alone or in combination with hydrogen peroxide. A saturated pre-ozonated solution, prepared with a low ozone demand water

(drinking water), was continuously mixed to the water to be treated before introduction of the reactive mixture in a nanofiltration unit (cross-flow filtration). The novelty of this work is also related to the use of organic membranes (made of polyethersulfone, PES, or polyamide, PA) whose the ozone compatibility has been addressed in a preliminary study [30]. The results emphasized that the PA membrane active layer was severely damaged by dissolved ozone whereas the PES matrix exhibited a fairly good resistance, even if the PVP additive was substantially degraded. Three micropollutants were investigated (deethylatrazine, DEA, carbamazepine, CBZ, and sulfamethoxazole, SMX) in the present study. However, most HONF experiments were carried out with drinking water spiked with DEA. This atrazine OTP is commonly detected in surface and ground waters. More importantly, DEA is a particularly effective $HO^{\bullet}$ radical probe characterized by a very low reactivity with O_3, which justifies its use in this study to track $HO^{\bullet}$ radicals in solution [33,34]. SMX and CBZ are pharmaceuticals with a high reactivity toward ozone, which are usually quickly oxidized by molecular ozone with concomitant slow formation of OTPs [35]. The degradation mechanisms of these two compounds are well described in the literature [36–39] and, consequently, their OTPs were not followed in this study.

2. Materials and methods

2.1. Experimental set-up description

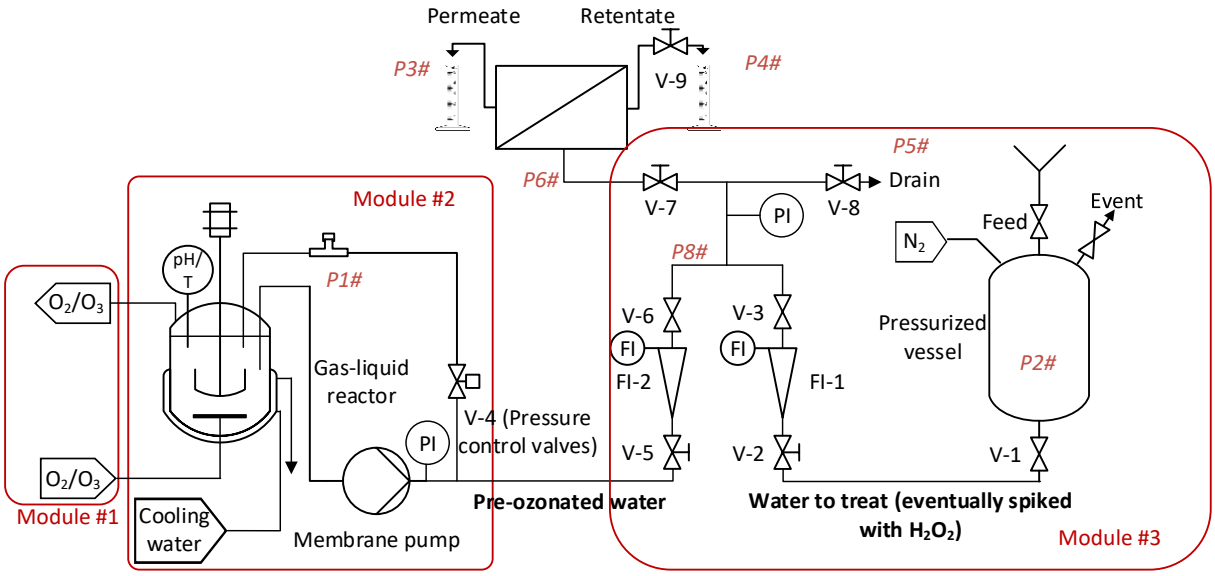

Figure 1: Process flow diagram of the experimental set-up.

In addition to the filtration cell described part 2.2, the experimental set-up was composed of three modules (Fig. 1) for the production of the pre-ozonated aqueous solution and its mixing with the studied water, possibly doped with H_2O_2. A picture of the experimental set-up is also available in the supplementary material (Fig. S1).

The first module (not detailed in Fig. 1), already described elsewhere [40], was devoted to the production of an ozone-enriched oxygen flow (at a concentration of 115 ± 2 gm^3 and a flow rate of 50 NL h^{-1}, under the normal conditions for temperature and pressure).

The second module was dedicated to the production of the saturated pre-ozonated aqueous solution. The ozone-enriched oxygen gas flow was continuously bubbled in 2 L of drinking water in a temperature-controlled gas-liquid reactor (supplied in Pyrex® by Cloup, France) equipped with a porous glass diffuser at the bottom and a mechanically agitated turbine. The pre-ozonated solution was continuously recirculated by a membrane pump (KNF, Germany). A pressure control valve V-4 (BP3, Go regulator, USA) allowed setting a controlled overpressure (up to 6 bar absolute) at the pump

discharge. The pre-ozonated aqueous solution was sampled at the port P#1, to quantify the dissolved ozone concentration at steady-state. The solution temperature and the pH within the gas-liquid reactor were continuously monitored using a pH/T combined probe provided by SI Analytics, connected to a WTW 315i pH-meter (Germany).

The third module contained a stainless steel 2 L tank (manufactured by Serv'Instrumentation, France) in which the studied water, possibly spiked with H_2O_2 and/or a micropollutant, was stored (Fig. S2 (b)). This tank was pressurized under inert gas (N_2), thus permitting a controlled water flow release toward the membrane unit. Flow rates of the pre-ozonated solution (F_2) and feedwater source (F1) were measured and controlled using two float-type flowmeters built with integrated control valves (FI-1 + V-2 and FI-2 + V-5, Brooks GT 1350, USA). Two valves (V-3 and V-6) were mounted downstream of the flowmeters to isolate each line. The pre-ozonated and water to treat solutions were continuously mixed just before the membrane unit (Part 2.2) in a T-shape fitting (Fig. S2 (a)). A control valve (V-7) was located before the membrane. A back-pressure valve located in the retentate line (V-9) allowed to set the transmembrane pressure (TMP) and retentate flow-rate during cross-flow filtrations. Typically, a permeate recovery rate (*RR*, defined in Table 1) of around 20% was implemented. The TMP was measured by a digital manometer (LEO 1 Keller, Switzerland). Except the by-pass line, which was composed of a PTFE tube (4mm inner diameter), stainless steel tubes (1/8 inch outer diameter) were used to avoid species adsorption.

Typically, a total feed flow rate of around 0.60-0.70L h^{-1} ($F_F = F_1 + F_2$) was targeted, trying to have a ratio F_2/F_F around 0.2 to minimize the intake of pre-ozonated solution. This range of flow rates leads to around 3 hours of service for each experiment considering the capacity of the storage vessel. The knowledge of the initial oxidants and MP concentrations (in P#1 for O_3 and P#2 for H_2O_2 and MP) before the mixing point (P#8, Fig. 1) and of the flow rates F_1 and F_2 enables to determine the concentration of the solutes in the feed solution ($C_{Oz,F}$, $C_{HP,F}$, $C_{MP,F}$) at the mixing point. The mixing efficiency at the mixing point was confirmed by assessing the ozone decomposition and radical generation at the membrane

cell inlet (Table S1 in supplementary material). Several criteria were determined to assess the performances of the hybrid process (Table 1). Each experiment was realized with a new compacted membrane (part 2.3).

Table 1: Criteria evaluated to assess the performance of the developed process.

Criteria	Equation	Unit	Reference
RR = Permeate recovery rate	F_P/F_F	-	[41]
R_i = Rejection rate of any species i	$1\text{-}C_{i,P}/C_{i,F}$	-	[41]
L_P = Permeability	$F_p/(S_m \times TMP)$	L h^{-1} m^{-2} bar^{-1}	
$\eta_{i,P}$ = removal yield of any species i in the permeate	$(C_{i,F} - C_{i,P})/C_{i,F}$		
$\eta_{i,R}$ = removal yield of any species i in the retentate	$(C_{i,F} - C_{i,R})/C_{i,F}$		
$\eta_{i,O}$ = overall removal yield of any species i	$(F_F \times C_{i,F} - F_R \times C_{i,R} - F_P \times C_{i,P})/(F_F \times C_{i,F})$		Based on the mass balance
$\{\int \boldsymbol{C_{HO^\bullet}dt}\}_{\boldsymbol{P}}$ = $HO^\bullet$ exposure in the permeate*	$= \frac{1}{k_{HO^\bullet}} \ln \frac{C_{DEA,F}}{C_{DEA,P}}$	mol L^{-1} s	[34]
$\{\int \boldsymbol{C_{HO^\bullet}dt}\}_{\boldsymbol{R}}$ = $HO^\bullet$ exposure in the retentate	$= \frac{1}{k_{HO^\bullet}} \ln \frac{C_{DEA,F}}{C_{DEA,R}}$	mol L^{-1} s	[34]
$\{\int \boldsymbol{C_{Oz}dt}\}_{\boldsymbol{R}}$ = O_3 exposure in the retentate	$= \frac{C_{Oz,F} + C_{Oz,R}}{2} \times (\tau_{in} + \tau_{ret})$	mol L^{-1} s	[42]
R_{ct}= Ratio of the $HO^\bullet$ exposure to the O_3 exposure in the retentate	$= \left\{\int \boldsymbol{C_{HO^\bullet}dt}\right\}_{\boldsymbol{R}} \Big/ \left\{\int \boldsymbol{C_{Oz}dt}\right\}_{\boldsymbol{R}}$		[33]

*The exposure to HO° was evaluated only when DEA was used because the other tested micropollutants have a high reactivity with molecular ozone and do not allow to track specifically hydroxyl radicals.

2.2. Filtration cell description

The tube length between the mixture point (P#8) and the membrane entrance was reduced as much as possible (35 cm) to limit the hydraulic residence time between these two points (τ_{in} estimated to 5 s at a flow rate of 600 mL h^{-1} recommended by the supplier to reach a cross-flow velocity of around 0.2 m s^{-1} within the cell). The cross-flow membrane unit (MemHPLC provided by MMS AG, Switzerland) was designed in stainless steel (description and pictures provided as supplementary material Part S2, Figs S3 and S4). Flat-sheet circular membrane coupons of 28 cm^2 (corresponding to a diameter of 6

cm) were installed in the cell. The hydraulic residence time of the retentate within the cell is estimated to around 5 s (τ_{ret}) at 600 mL h^{-1}.

2.3. Membranes description and preparation

A commercial flat-sheet NF membrane (NP10) supplied by Microdyn Nadir (Germany) was mainly used in this study. The active layer of the membrane is made of polyethersulfone (PES) and polyvinylpyrrolidone (PVP). It has a molecular weight cut-off (MWCO) of 1000-1200 Da. Before the first use, the membrane coupons were cleaned to remove potential preservative agents according to the following protocol: sonication in a 50/50 (v/v) water/ethanol mixture followed by rinsing with pure water and sonication (twice for 2 min).

A thin-film composite (TFC) polyamide (PA) membrane (NF270 from Dow Filmtech), having a lower MWCO (200-300 Da) than the PES membrane, was also considered in the experiments carried out with river water. Before the first use, the PA membrane coupons were cleaned with the same protocol than the PES membrane, except that only pure water was used.

After cleaning, all membrane coupons were stored in pure water at 4°C. To avoid bacterial proliferation, the water was changed every two days. The membrane coupons were compacted directly in the MemHPLC cell (cross-flow mode) at a TMP of 6 bar, using pure water introduced in the pressurized vessel (P#2) until the permeability remained constant (typically 10-15 h for the PES membrane and 4 h for the PA membrane).

2.4. Membrane characterization by ATR-FTIR

The exposed membranes were thoroughly rinsed with deionized water to remove reversible fouling and were stored in pure water at 4°C for further characterization. The water was renewed every two days. To monitor the changes in functional groups of the membranes, Fourier transform infrared (FTIR) spectra were acquired in attenuated total reflectance (ATR) mode using an infrared spectrometer (Perkin Elmer) equipped with a diamond crystal ATR element (single reflection; angle:

45°). Each spectrum was averaged from 20 scans collected from 650 to 4000 cm^{-1} at a 2 cm^{-1} resolution. Membrane samples were vacuum-dried for two days prior to analysis.

2.5. Chemicals and analytical methods

MP (provided by Sigma-Aldrich) were all of analytical grades. Hydrogen peroxide (35% in water) was purchased from Acros-Organics. The main physico-chemical properties of the oxidants and MP used are summarized in Table 2.

Table 2: Main physico-chemical properties of the solutes involved in this study.

Solute	*M*	*pKa* at 20°C	Water solubility	Charge at 7 ≤ pH ≤ 8	Log K_{ow}	$k_{i,HO}$	$k_{i,Oz}$	References
	g mol^{-1}		mg L^{-1}			L mol^{-1} s^{-1}	L mol^{-1} s^{-1}	
H_2O_2	34.01	11.75	Soluble	neutral			2.40×10^6 with HO_2^-	[43,44]
DEA	187.6	1.3-1.65	3200	negative	1.52	1.2×10^9	0.18	[34,45]
CBZ	236.3	14	17.7 at 25°C	neutral	2.25	8.8×10^9	3×10^5	[46,47]
SMX	253.3	1.6 / 5.7	281 at 25°C	Negative (two charges)	0.89	5.5×10^9	2.5×10^6	[48–51]
O_3	48.0			neutral		2×10^8-2×10^9		[52,53]

Ozone, hydrogen peroxide and micropollutant concentrations were quantified at the feed inlet and at both the permeate and retentate outlets. An excess of sodium thiosulfate powder was used to quench the oxidants in the vials in which samples for MP quantification were collected. MP quantification was achieved with a Waters 996 High Performance Liquid Chromatography equipped with a Waters 996 PDA (Photodiode Array Detector) and a Waters 600 LCD pump. The separation was conducted on a column Waters C-18 (5 µm; 4.6 × 250 mm). Samples were analyzed after filtering through a 0.2 µm membrane filter. The calibration curves equations and statistics, as well as limits of detection and quantification (LOD and LOQ) are provided in Table S.2.

The H_2O_2 concentration was quantified by the iodometric method in which iodide is catalytically oxidized in iodine at acidic pH [54]. An excess of glycine was introduced in the sampling vials when

ozone was suspected to be present to selectively quench the ozone residual. The iodine titration by sodium thiosulfate was carried out right after the sampling.

The ozone concentration was selectively quantified by the Indigo method [55]. A Helios UV–Vis spectrophotometer (Shimadzu, Japan) was used for the indigo absorbance measurement, performed a few minutes after the sampling (λ = 600 nm). The ozone decomposition involved in the dead volume located between the sampling point (P#1) and the mixture point has been taken into account (Part S5 in supplementary material).

2.6. Water characteristics

Two water matrices were studied: (i) the drinking water from the city of Rennes in France (pH = 8.05, alkalinity = 1.7 mmol of $HCO_3^-L^{-1}$, dissolved organic carbon (DOC) = 2.4 ppm) and (ii) a surface water sampled in the Vilaine river (Rennes, France) in February 2021. The Vilaine water was settled and filtrated prior use at 0.45 µm (pH = 7.9, alkalinity = 1.4 mmol of HCO_3^- L^{-1}, dissolved organic carbon (DOC) = 10 ± 2 ppm). These two water matrices were synthetically polluted by known amounts of MP previously dissolved in stock solutions of ultrapure water.

3. Results and discussion

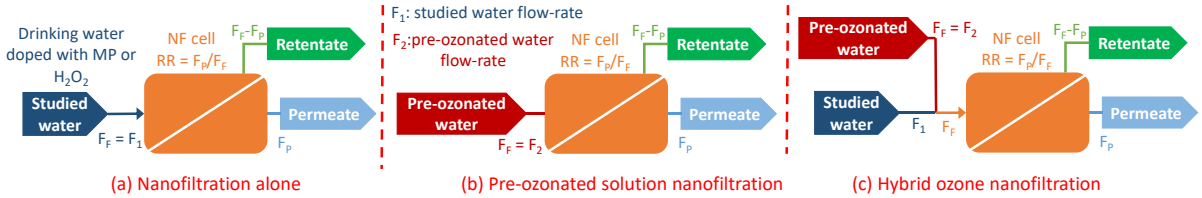

Figure 2: Description of the different configurations investigated.

Prior to the assessment of HONF without (part 3.3) and with H_2O_2 (parts 3.4 and 3.5), regular MP and H_2O_2 nanofiltration experiments (Figure 2 (a)) were undertaken to determine the rejection performance in an unreactive configuration (part 3.1). The nanofiltration of the pre-ozonated aqueous solution (Fig. 2 (b)) alone is considered separately (part 3.2) owing to the intrinsic ozone-self decomposition [16].

3.1. Performance of nanofiltration alone for the micropollutants and H_2O_2 rejection

3.1.1 Micropollutants rejection

Table 3: H_2O_2, DEA, CBZ, SMX nanofiltration in drinking water at steady-state using the NP10 PES membrane (Fig. 2(a)). Experimental conditions: TMP = 5 bar, filtration time = 3 h, T = 19.5 ± 0.5°C.

Compound	Config.	F_F	RR	$C_{i,F}$	R_j	L_p
		L h^{-1}		mg L^{-1}		L h^{-1} m^{-2} bar^{-1}
H_2O_2	Cross-flow	625	20.5 ± 1.0 %	4.59	3.40 ± 0.06 %	9.2 ± 0.3
DEA	Cross-flow	578	20.3 ± 0.7 %	0.204	13.0 ± 0.4 %	8.4 ± 0.1
DEA	Dead-end	121		0.194	8.7 ± 0.4 %	8.6 ± 0.1
DEA	Cross-flow	555	20.0 ± 0.8 %	11.8	9.2 ± 0.1 %	7.9 ± 0.1
DEA	Dead-end	115		13.9	5.3 ± 0.1 %	8.2 ± 0.1
CBZ	Cross-flow	521	22.3 ± 0.8 %	0.195	19.0 ± 0.6 %	8.3 ± 0.2
CBZ	Dead-end	118		0.195	18.1 ± 0.9 %	8.4 ± 0.2
SMX	Cross-flow	542	19.8 ± 0.4 %	0.207	20.6 ± 0.4 %	7.7 ± 0.1
SMX	Dead-end	107		0.207	18.0 ± 0.7 %	7.6 ± 0.4

DEA, CBZ and SMX removal by filtration alone (Fig. 2(a)) have been measured using both cross-flow and dead-end configurations (Table 3) with the NP10 PES membrane. Both the membrane permeability and the rejection rate remained constant over time, showing that doped drinking water had a low membrane fouling capacity.

In NF, solute rejection by the membrane results from the complex interplay between steric and electrostatic effects [5]. On the one hand, considering the molecular weight of the solutes selected in this study (in the range 187.6 (DEA) to 253.3 (SMX) g mol^{-1}) and the NP10 membrane MWCO (1000-1200 g mol^{-1}), a low steric rejection was expected. On the other hand, DEA and SMX (Table 1) exist at their negatively charged state at the pH under consideration, which could contribute to increase their rejection [9,10]. However, it can be seen in Table 3 that MP elimination by the membrane alone is low (3-20%) whatever the molecule, suggesting the prevalence of convective transfer through the membrane on electrostatic repulsions. It is worth noting that no solute adsorption was detected on the membrane surface by ATR-FTIR, which is not surprising due to the low solute concentration in the feed solutions.

It can also be observed that the solutes rejection is higher in cross-flow mode compared to dead-end mode (Table 3). During filtration, rejected solutes tend to accumulate at the membrane/fluid boundary layer (the so called “concentration polarization” phenomenon) and are thus prone to diffusive transfer through the membrane [9]. In cross-flow mode, the concentration polarization phenomenon is reduced compared to dead-end mode due to the occurrence of a tangential velocity shearing-off rejected molecules from the membrane surface and thus reducing the risk of diffusive transfer through the membrane. The same phenomenon might be responsible for the better rejection observed for the less concentrated DEA solution (0.204 ppm) compared to the higher one (11.8 ppm). Thus at higher concentration, more compounds are accumulated in the concentration polarization layer, which favors diffusive transfer.

3.1.2 H_2O_2 rejection

H_2O_2 rejection by the PES membrane was also assessed without ozone using the cross-flow configuration and drinking water (Fig. 2(a)). H_2O_2 rejection rate was almost negligible (3.4%) owing to its low molecular weight. Both the membrane permeability and the rejection rate remained constant over time. In order to assess the impact of low concentration of H_2O_2 (a few ppm) on membrane stability, the membranes have been characterized by ATR-FTIR and no significant modification of the membrane surface chemistry has been observed between the pristine membrane and those that were exposed to H_2O_2 (Figure S7 in supplementary material) in agreement with the study reported by Li *et al.* (2019). Another study assumed that the exposure of PES membranes to H_2O_2 might lead to the modification of the filtration performance and to their accelerated ageing [57]. However, this hypothesis was based on the literature related to PES-membrane exposure to sodium hypochlorite and was not supported by any material surface chemistry analysis. Furthermore, it is worth noting that the membranes were exposed to high concentrations of H_2O_2 (1-5 wt%) unlike the present study.

3.2 Pre-ozonated solution nanofiltration

Table 4: Pre-ozonated solution nanofiltration (prepared with drinking water) using NP10 PES membrane (Fig. 2(b)). Experimental conditions: TMP = 5 bar, F_F = 240 mL h^{-1}, RR = 43%, filtration time = 1 h, T = 19.5 ± 0.5°C.

$C_{Oz,F}$	$C_{Oz,P}$	$C_{Oz,R}$	$\eta_{Oz,P}$	$\eta_{Oz,R}$	L_p at t_0
mg L^{-1}	mg L^{-1}	mg L^{-1}	%	%	L h^{-1} m^{-2} bar^{-1}
15.5	0.2 ± 0.1	12.7 ± 0.2	98.5	18.1	9.3 ± 0.3

The behavior of O_3 during NF in the cross-flow configuration has been investigated using only the pre-ozonated solution (Fig. 2(b)), without mixture with the solution to be treated (Table 4). On the one hand, the ozone concentration in the retentate was 18% lower than the feed concentration. According to the low liquid residence time in the retentate side (τ_{ret} around 11 s in that case), this ozone decomposition cannot be attributed to only the inherent ozone-self decomposition in drinking water

(Part S5). It emphasizes that O_3 diffused to the membrane surface and reacted with it. Indeed, Ouali et al. (2021) demonstrated that the PVP additive was particularly sensitive to ozone [30]. On the other hand, the ozone concentration was negligible in the permeate. With a molecular weight much lower than the MWCO of the PES membrane, this result cannot be attributed to steric rejection and highlights that full O_3 decomposition may occur within the pores of the membrane leading to the generation of surface radicals [30] and degradation of the membrane structure. Indeed, during the experiment, the TMP and the permeate flow rate decreased and increased quickly, respectively, after a few minutes of operation. It is worth noting that the membrane degradation was too fast to monitor these variations.

The potential reaction of O_3 with the PVP additive was confirmed by ATR-FTIR (Figure S8): the decrease in intensity of the PVP band (1668 cm^{-1}) and its broadening indicate significant degradation of the PVP. Moreover, the new band appearing at 1035 cm^{-1} can be assigned either to the formation of strong sulfonic acids resulting from PES chain scission and/or to the formation of phenol groups (hydroxylation of the PES aromatic rings) [58,59].

Thus, filtration of the pre-ozonated aqueous solution confirmed the low ozone compatibility of polymeric membranes. Parts 3.3 to 3.5 are dedicated to HONF with the developed monophasic configuration (Fig. 2(c)), in which a fast ozone decomposition is expected right after the mixing of the studied water with the pre-ozonated solution [42], which should mitigate the ozone diffusion toward the membrane surface.

3.3 Monophasic hybrid-ozone membrane filtration of drinking water non-doped with H_2O_2

The monophasic hybrid process (mixture of a pre-ozonated solution with the water to be treated at the membrane cell inlet) was first evaluated without H_2O_2 added (Fig. 2(c)). During this experiment, the permeability increased over time (Table 5), from 9.9 to 12.9 L h^{-1} m^{-2} bar^{-1} in less than 30 min, proving that, with this configuration, the membrane was still altered by the reaction with O_3 and/or

radicals formed during the ozone decomposition. It shows that even if a fast ozone decomposition was expected after the mixing point due to fast reactions with some moieties of the natural organic matter and some inorganic anions [32,42,60], a significant amount of ozone still diffused to the membrane surface and eventually penetrated within the membrane pores. No dissolved ozone residual was detected in the permeate (Fig. 3(a)). Besides, the permeability increase was slower than in section 3.2, in which only a pre-ozonated solution was filtered. These two features demonstrate that the mixture between the pre-ozonated solution and the studied water enabled to lower the dissolved ozone exposure ($\int C_{oz} dt$, defined Table 1), and thus to lower the dissolved ozone concentration at the membrane surface.

Interestingly, even if the membrane was degraded, the ozone and DEA concentrations remained constant over time in both the permeate and retentate. Overall ozone and DEA removal yields equal to 82 and 47%, respectively, were measured (Fig. 3 (a) and (b)). More precisely, in the permeate, the DEA removal yield was equal to 55%. These constant removal yields over time are consistent with the high MWCO of the NP10 membrane (Part 3.1). Consequently, the variations of the ozone and DEA concentrations between the feed and both the permeate and retentate were mainly governed by oxidation reactions, not membrane rejection. The R_{ct} (Table 1), which represents the ratio of the hydroxyl radical exposure to the ozone exposure [33], was estimated in the retentate, considering that solute rejection was negligible with the PES membrane (Fig. 4 (a) and (b), Table 5). Thus, its value was particularly high (2.1×10^{-6}), around two orders of magnitude higher than with other traditional ozone based AOPs [12,14,33,61], showing that the fast ozone decomposition observed at a low reaction time of a few seconds is combined to a particularly high radical generation. This R_{ct} value is even one or two order of magnitude higher than the values reported by Biard *et al.* (2018) using a similar monophasic configuration in a tubular reactor (*i.e.* without membrane filtration). It might be due to additional oxidation reactions between ozone and the membrane surface (for example with the PVP additive) and/or with the NOM concentrated in the boundary layer at the membrane surface leading to the formation of more radicals.

HONF of the drinking water was repeated with the addition of tert-butanol, a radical scavenger [12,62], introduced in excess at a concentration of 0.01 M (Table 5). On the one hand, both the O_3 (from 78 to 12%) and DEA (from 55 to 22%) removal yields significantly decreased in the retentate in this experiment compared to the reference experiment without radical scavenger. It confirms that both the ozone decomposition and radical generation rate were slow down owing to the radical scavenger, and that free radicals are involved in this side of the membrane without tBuOH. As a consequence, the radical exposure and the R_{ct} decreased by factors three and five, respectively (Fig. 4 (a) and (b)). Nonetheless, the R_{ct} value remained high in the retentate (around 4×10^{-7}), which is unlikely with the addition of a free radical scavenger [62], confirming that ozone reactions with the membrane surface in the retentate side might be also involved, leading probably to surface radicals generation. On the other hand, η_{DEA} (49%) in the permeate during this experiment was higher than for the reference experiment (Fig. 4(b)). η_{Oz} was still also very high (around 90%). These two features confirm that other radicals, probably surface radicals not scavenged by tBuOH, generated from the reaction of O_3 with the membrane (part 3.2), might be also involved within the membrane pores. Surprisingly, during this experiment, no significant evolution of the permeability was observed after 2 h of experiments, demonstrating that the membrane, even if it is involved in chemical reactions, is not significantly altered at this time scale with tBuOH. A possible explanation is that the reactions involved in this case might be not destructive (catalytic action) whereas the free radicals generated in the liquid bulk might be able to damage severely the membrane [30].

Whatever, due to the fast membrane degradation observed without H_2O_2, this configuration was gave up for the rest of the study.

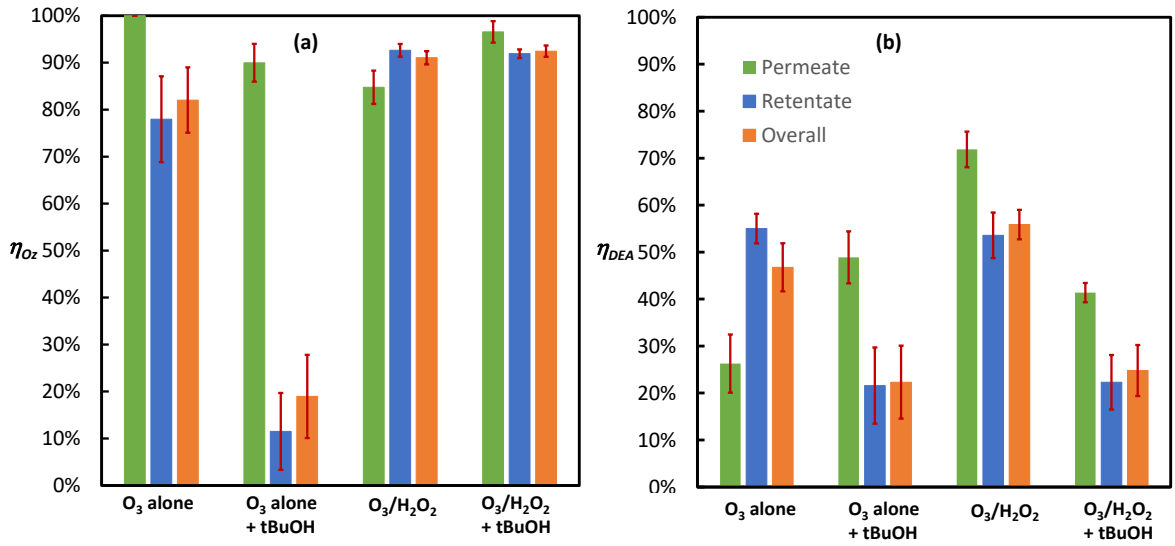

Figure 3: Comparison of the ozone(a) and DEA (b) removal efficiencies (in the permeate (green), in the retentate (blue) and overall (orange)) using the hybrid ozone nanofiltration for the drinking water with O_3 alone, O_3 alone + tBuOH (0.01M), with O_3/H_2O_2 and with O_3/H_2O_2 + tBuOH (0.01M).

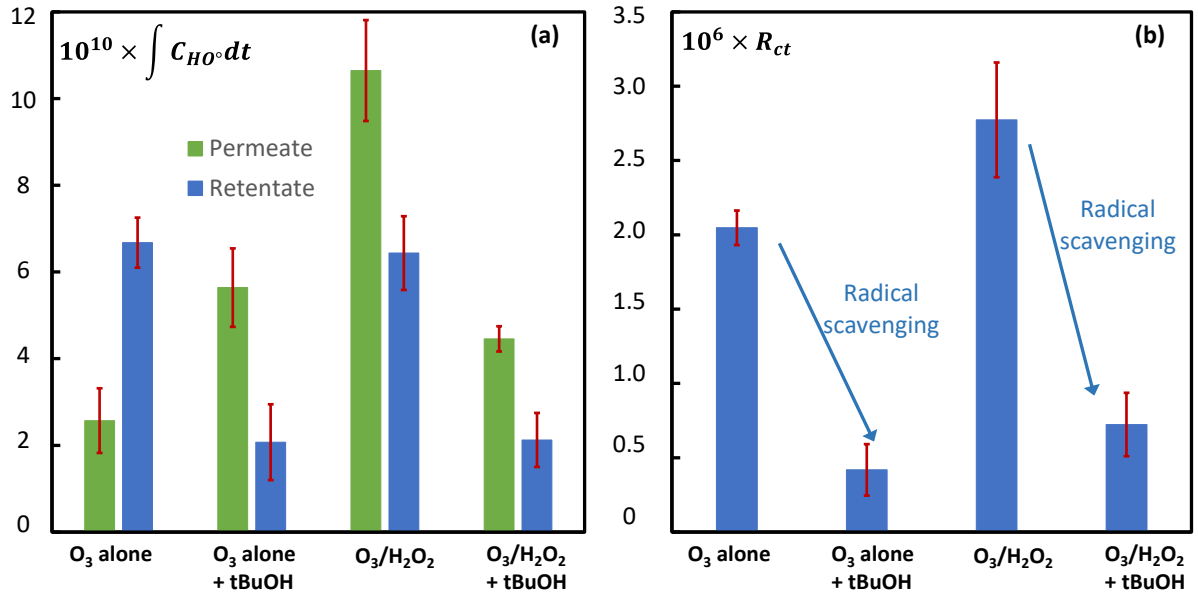

Figure 4: Comparison of the $HO^\bullet$ exposure (a) and of the R_{ct} (b) (in the permeate (green) and in the retentate (blue)) using the hybrid ozone nanofiltration for the drinking water with O_3 alone, O_3 alone + tBuOH (0.01M), with O_3/H_2O_2 and with O_3/H_2O_2 + tBuOH (0.01M).

Table 5: Monophasic hybrid-ozone membrane filtration (NP10 PES membrane) of drinking water non-doped with H_2O_2 (F_F=660 mL h^{-1}, F_2/F_F≈ 0.22, $C_{oz,F}$≈ 2.5 ppm, $C_{DEA,F}$ ≈ 0.15 ppm)

MP	*RR*	$\eta_{Oz,P}$	$\eta_{DEA,P}$	L_p	$\{\int C_{HO^\circ} dt\}_P$	$\eta_{Oz,R}$	$\eta_{DEA,R}$	$\{\int C_{HO^\circ} dt\}_R$	R_{ct}	$\eta_{Oz,O}$	$\eta_{DEA,O}$
	%	%	%	L h^{-1} m^{-2} bar^{-1}	mol L^{-1} s	%	%	mol L^{-1} s		%	%
DEA	20 ± 3	100	26 ± 6	Increased with *t*	(2.6 ± 0.7)×10^{-10}	78 ± 9	55 ± 3	(6.7 ± 0.6)×10^{-10}	(2.1 ± 0.1)×10^{-6}	82 ± 7	47 ± 5
DEA + tBuOH (0.01 M)	12.2 ± 0.7	90 ± 4	49 ± 6	7.0 ± 0.5	(5.6 ± 0.9)×10^{-10}	12 ± 8	22 ± 8	(2.1 ± 0.9)×10^{-10}	(0.4 ± 0.2)×10^{-6}	19 ± 9	22 ± 8

Table 6: Monophasic hybrid-ozone membrane filtration (NP10 PES membrane) of drinking water doped with H_2O_2 (F_F = 660 mL h^{-1}, F_2/F_F≈ 0.22, $C_{oz,F}$≈ 2.5 ppm, $C_{DEA,F}$ ≈ 0.15 ppm, 3.5 h of experiment, TMP = 4.2 bar)

MP	$C_{HP,F}/C_{Oz,F}$	*RR*	$\eta_{Oz,P}$	$\eta_{MP,P}$	$\left\{\frac{\Delta C_{HP}}{C\Delta C_{Oz}}\right\}_P$	L_p	$\{\int C_{HO^\circ} dt\}_P$	$\eta_{Oz,R}$	$\eta_{MP,R}$	$\left\{\frac{\Delta C_{HP}}{C\Delta C_{Oz}}\right\}_R$	$\{\int C_{HO^\circ} dt\}_R$	R_{ct}	$\eta_{Oz,O}$	$\eta_{MP,O}$	$\left\{\frac{\Delta C_{HP}}{C\Delta C_{Oz}}\right\}_O$
	mol mol^{-1}	%	%	%	mol mol^{-1}	L h^{-1} m^{-2} bar^{-1}	mol L^{-1} s	%	%	mol mol^{-1}	mol L^{-1} s		%	%	mol mol^{-1}
DEA	1.56	17.9 ± 0.9	85 ± 4	72 ± 4	0.81 ± 0.09	10.3 ± 0.7	(1.1 ± 0.1)×10^{-9}	93 ± 2	54 ± 5	0.64 ± 0.04	(6.4 ± 0.9)×10^{-10}	(2.8 ± 0.4)×10^{-6}	91 ± 2	56 ± 3	0.64 ± 0.4
DEA + tBuOH (0.01 M)	1.39	21 ± 1	97 ± 2	41 ± 2	0.59 ± 0.08	12.6 ± 0.4	(4.5 ± 0.3)×10^{-10}	92 ± 1	22 ± 6	0.6 ± 0.2	(2.1 ± 0.6)×10^{-10}	(0.7 ± 0.2)×10^{-6}	92 ± 2	25 ± 6	0.6 ± 0.1
CBZ	0.84	10.0 ± 0.6	86 ± 2	> 90%*	0.42 ± 0.03	4.8 ± 0.4		93 ± 3	> 90%	0.33 ± 0.01			92 ± 3	> 90%	0.36 ± 0.02
SMX	1.18	20 ± 1	94 ± 1	> 95%	0.61 ± 0.03	11.0 ± 0.7		96 ± 2	> 95%	0.54 ± 0.04			96 ± 1	> 95%	0.57 ± 0.03

*The CBZ and SMX concentrations in both the permeate and retentate were lower than the detection limit (Table S2). Consequently, removal efficiencies are higher than the one calculated taking into account the detection limits.

Table 7: Monophasic hybrid-ozone membrane filtration (NP10 PES and NF270 PA membranes) of the river water sample doped with H_2O_2 and DEA (F_F = 635 mL h^{-1}, F_2/F_F≈ 0.21, $C_{oz,F}$≈ 3.8 ppm, $C_{DEA,F}$ ≈ 0.16 ppm, 3 h of experiment, TMP = 4.9 bar)

Membrane	$C_{HP,F}/C_{Oz,F}$	O_3 dose	RR at t_0	$\eta_{Oz,P}$	$\eta_{DEA,P}$	$\eta_{DOC,P}$	$\left\{\frac{\Delta C_{HP}}{C\Delta C_{Oz}}\right\}_P$	$\{\int C_{HO^\circ}dt\}_P$	$\eta_{Oz,R}$	$\eta_{DEA,R}$	$\eta_{DOC,R}$	$\left\{\frac{\Delta C_{HP}}{C\Delta C_{Oz}}\right\}_R$	$\{\int C_{HO^\circ}dt\}_R$	R_{ct}	$\eta_{Oz,O}$	$\eta_{DEA,O}$	$\eta_{DOC,O}$	$\left\{\frac{\Delta C_{HP}}{C\Delta C_{Oz}}\right\}_O$
	mol mol^{-1}	g_{O3} g^{-1}_{DOC}	%	%	%		mol mol^{-1}	mol L^{-1} s	%	%		mol mol^{-1}	mol L^{-1} s		%	%		mol mol^{-1}
NP10	0.94	0.31	20.5	99.3±0.7	35±5	36 ± 2	0.4± 0.1	(3.7± 0.8)×10^{-10}	97± 2	16± 7	20 ± 5	0.43± 0.08	(1.5± 8)×10^{-10}	(4± 2)×10^{-7}	97± 2	20± 6	22± 5	0.41± 0.9
NF 270	0.81	0.56	20.5	100	70±3	69±8	0.16± 0.05	9.7± 0.8)×10^{-10}	97± 1	14± 4	-9 ± 6	0.21± 0.02	(1.25± 0.4)×10^{-10}	(2.8± 0.9)×10^{-7}	97± 2	26± 5	8± 6	0.25± 0.05

3.4 Monophasic hybrid-ozone membrane filtration doped with H_2O_2 using the NP 10 PES membrane

3.4.1 Application to drinking water doped with DEA

In agreement with the study of Biard *et al.* (2018), an equimolar ratio ($C_{HP,F}/C_{oz,F} \approx 1$) of hydrogen peroxide and ozone was targeted at the mixing point to assess HONF of drinking water with the peroxone process (Fig. 2(c)). This ratio was optimal to enhance the ozone decomposition and the radical generation and to limit at the same time the H_2O_2 dose required [42]. The overall consumption ratio of H_2O_2 over O_3 ($\Delta C_{HP}/\Delta C_{Oz}$) remained in the expected range [42], close to 0.5 mol mol^{-1} (Table 6). Contrarily to the experiment without H_2O_2 (part 3.3), no significant variation of the membrane permeability was observed over time, even if a slight broadening and decrease of the PVP band intensity (1668 cm^{-1}) was noticed (Figure 5).

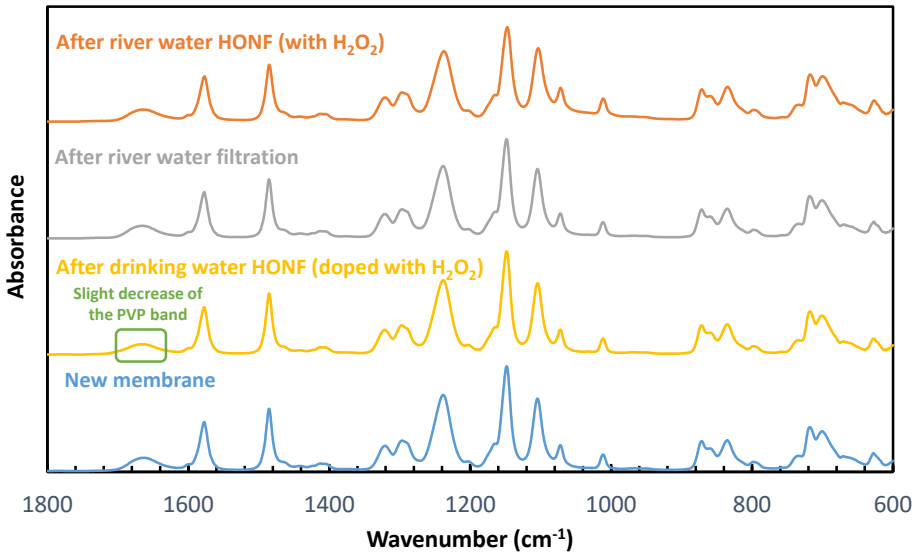

Figure 5: ATR-FTIR spectra of new and exposed NP10 membranes.

The overall η_{Oz} was equal 91% with H_2O_2 (Figure 3(a)). Thus, as expected, the addition of H_2O_2 enhanced the initiation of the ozone decomposition in the liquid bulk before entrance in the membrane cell [15], allowing to decrease the dissolved ozone exposure ($\int C_{oz}dt$) [17], which should be advantageous to limit the ozone diffusion at the membrane surface. This enhancement of the ozone decomposition rate is

concomitant with a higher overall DEA removal yield of 56%, which is promising considering that DEA has also a rather low reaction rate constant with hydroxyl radicals of 1.2×10^{9} L mol^{-1} s^{-1} in comparison with many other micropollutants [34,63] (Figure 3(b)). It is also worth noting that this removal yield was obtained despite the relatively high MWCO of the membrane considered here (1000 – 1200 Da) compared to the DEA molecular weight (187.6 $g.mol^{-1}$).

More precisely, in the retentate, the removal yields are not significantly different with and without H_2O_2 (Fig. 3(b)), which highlights similar hydroxyl radical exposures (Fig. 4(a)) [17]. Nonetheless, owing to a lower ozone exposure, the R_{ct} value in the retentate (Figure 4(b)) was particularly high (2.8×10^{-6}), and increased by 33% compared to the experiment without H_2O_2. It confirms that using the peroxone process, most of the ozone might be decomposed before going into contact with the membrane, which might be responsible for the main generation of free radicals in solution. On the contrary, using only ozone, a significant part of O_3 might be able to reach the membrane surface to form surface radicals, leading to similar oxidation performance but also to a detrimental membrane degradation (part 3.3).

In the permeate, the DEA removal yield was even better (72%) than in the retentate. It could be due to reactions of the low dissolved ozone residual within the pore with either H_2O_2 or the membrane surface. Anyway, it did not lead to significant membrane degradation as the permeability remained constant during the experiment. Thus, an $HO^{\bullet}$ exposure around one order of magnitude higher than without H_2O_2 was measured (Figure 4(a) and Tables 5 and 6). This value must not be considered as a real estimation of the $HO^{\bullet}$ exposure but more as an indirect evaluation of the extent of MP degradation in the permeate because other type of radicals might be involved owing to the membrane.

The addition of a radical scavenger (tBuOH) in the water to be treated did not influence the ozone decomposition significantly (Fig. 3(a)) owing to the fact that O_3 reacts mainly with H_2O_2 in the drinking water. Nonetheless, the free radicals generation was clearly inhibited, with lower DEA removal yield (Fig. 3(b)), $HO^{\bullet}$ exposure and R_{ct} (Fig. 4). It confirms the prevalence of the free hydroxyl radical route using the peroxone process. Nonetheless, the R_{ct} was still of the order of magnitude of 10^{-7}, showing

that additional surface radicals able to react with DEA were nevertheless also involved in that particular case.

3.4.2 Application to two pharmaceuticals

DEA has a very low reaction rate constant with ozone (Table 2). Thus, its degradation involved mainly $HO^{\bullet}$ radicals, not molecular ozone. However, many micropollutants are electron-rich species and have higher reaction rate constants with O_3, especially many pharmaceuticals [50], such as SMX and CBZ (Table 2), which means that they are predominantly oxidized by molecular ozone, not hydroxyl radicals [17]. Nonetheless, even if the addition of H_2O_2 allow to drastically decrease the ozone exposure at a constant ozone dose by lowering ozone lifetime, these two compounds are well degraded, with concentrations in the permeate and retentate lower than the detection limits (Table 6). It demonstrates that high removal efficiencies are also feasible in the retentate allowing to pretreat the membrane concentrate. As expected, the ozone decomposition was not affected by the nature of the micropollutants added in the water (Tables 6), but should depend only on the nature of the water and the hydrogen peroxide dose [42].

3.4.3 Influence of the water matrix: application to a river water

Drinking water used previously is characterized by a low organic matter concentration and a low fouling potential (part 3.1). The water matrix considered in this part is more challenging as raw river waters are characterized by a higher fouling potential compared to drinking water.

Figure 6(a) enables to compare the permeabilities against time of the PES membranes in the river water during simple nanofiltration and during HONF with H_2O_2 addition (Table 7). The results clearly highlight that the permeabilities decreased significantly over time and confirm that the river water had a high fouling potential. Thus, without oxidant, the permeability decreased by around 40% after one hour of operation. Nonetheless, the permeability decreased advantageously by only ~25% with the hybrid process after one hour showing that it allows to mitigate membrane fouling.

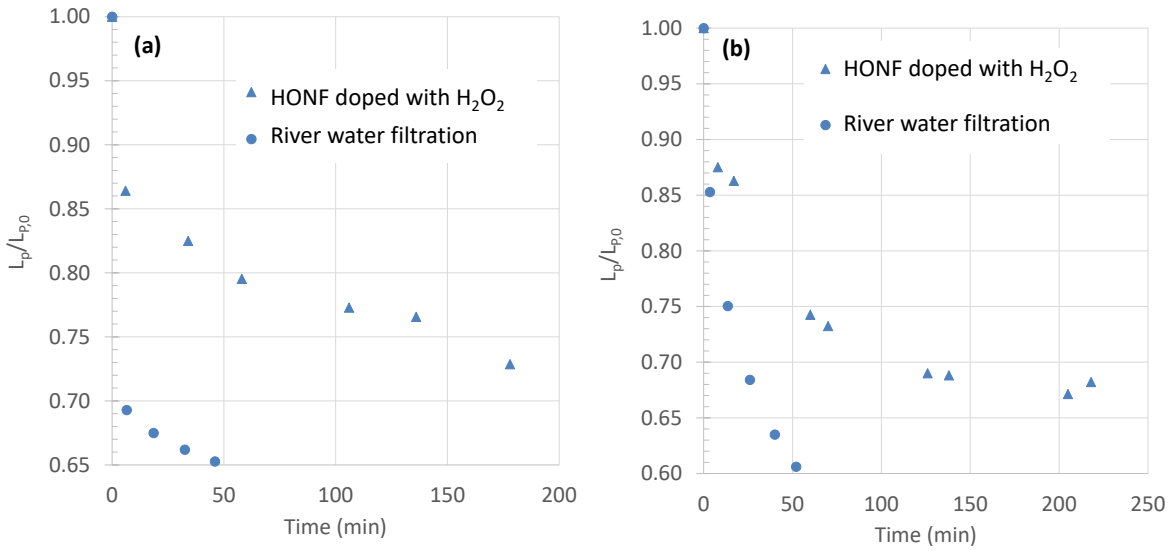

Figure 6: Ratio of the membrane permeability over the membrane permeability at t_0 vs. filtration time during simple nanofiltration of river water (no oxidant, circles) and during HONF of the river water doped with H_2O_2 (triangle) for the NP10 PES (a) and NF270 PA (b) membranes.

O_3 was almost entirely consumed in both the permeate and retentate (Figure S6 and Table 7), which can be attributed to a fast ozone decomposition induced by its reactions with H_2O_2 and with some moieties of the NOM present at high concentration in the river water [32]. This fast ozone decomposition rate is particularly interesting to lower the ozone exposure ($\int C_{oz}dt$), *i.e.* to decrease the ozone lifetime in solution and eventually to decrease the ozone diffusion at the membrane surface [17]. This behavior is confirmed by the fact that no significant modification of the ATR-FTIR spectra (Figure 5) was observed after HONF of the river water demonstrating that, in that case, no dissolved ozone residuals and radicals reach the membrane surface of the membrane pores. Nonetheless, the overall DEA removal yields were lower in both the permeate (35%) and retentate (16%) than with the drinking water (Figure 3(b) and 7(b)), resulting from lower radical exposures (Fig. 8(a)). Thus, R_{ct} values were one order of magnitude lower (order of magnitude of 10^{-7}) even if they remain quite high, showing a lower availability of free hydroxyl radicals than in drinking water (Fig. 8(b)). It indicates that NOM may play also the role of inhibitor by scavenging radicals involved in the ozone decomposition [62]. The overall DOC removal yield was around 22% and indicates that a part of the DOC was

mineralized (Fig. 7(a)). The retentate concentration was higher than the permeate concentration, which can be due to a higher oxidation rate and/or to membrane rejection.

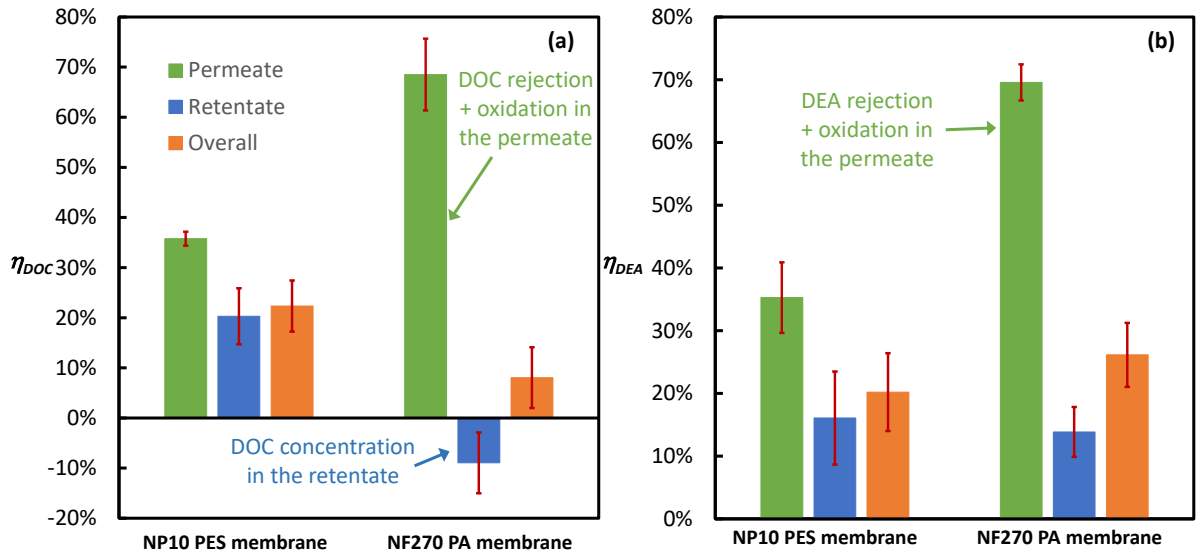

Figure 7: Comparison of the DOC (a) and DEA (b) removal efficiencies (in the permeate (green), in the retentate (blue) and overall (orange)) using the hybrid ozone nanofiltration (O_3/H_2O_2) for the river water with the two membranes.

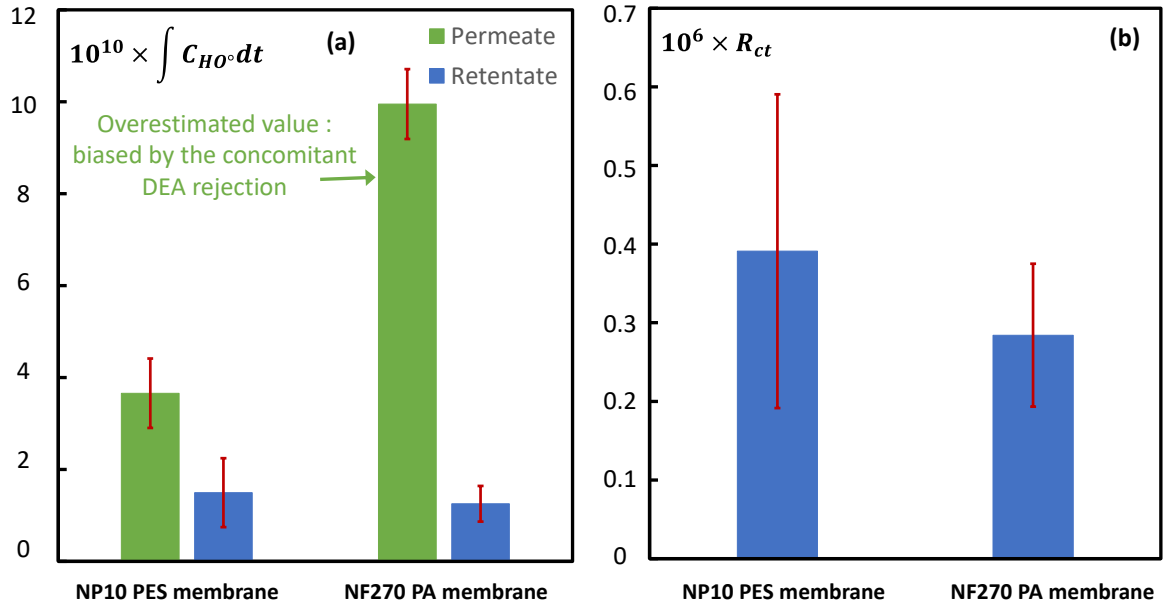

Figure 8: Comparison of the $HO^\bullet$ exposure (a) and of the R_{ct} (b) (in the permeate (green) and in the retentate (blue)) using the hybrid ozone nanofiltration (O_3/H_2O_2) for the river water with the two membranes.

3.5 River water HONF using the NF270 PA membrane

In the parts 3.1 to 3.4, the PES membrane was selected because of its relatively high resistance to oxidation. In this part, the study was enlarged to the NF270 polyamide membrane to better assess the robustness of this hybrid operation with the river water. Indeed, PA membrane are usually tighter (lower MWCO) but also less resistant to O_3 [30].

The observed ozone and DEA overall removal yields were close to the one measured with the PES membrane with the same water matrix, which shows that the reactions involved are not influenced by the membrane nature (Figures S6 and 7(b), Table 7). It confirms that using the river water sample doped with H_2O_2, the chemical reactions involved are mainly located in the liquid bulk, not at the membrane surface. It leads to similar R_{ct} whatever the membrane used (Fig. 8(b)). The DEA removal yield in the permeate (70%) is particularly higher than in the retentate (14%), which shows that using the tighter NF270 PA membrane (200-300 Da), DEA rejection is combined to its chemical oxidation. Thus, the value of the radical exposure ($\int C_{HO^\bullet} dt$) reported is biased (Table 7 and Fig 8(a)) and overestimates the real value.

This synergy between the oxidation and filtration processes is confirmed by the DOC removal yields. Indeed, the DOC concentration in the retentate is higher than in the feed solution ($\eta_{DOC,R}$ of -9%) which results from rejection effects. Still, the overall η_{DOC} is low (8%) and consistent with the applied ozone dose of 0.56 $g_{Oz}\ g_{DOC}^{-1}$. It is noteworthy that application of ozonation processes in water treatment are not dedicated to DOC mineralization.

With the hybrid process, the permeabilities decreased by only ~20% in one hour compared to ~40% during a simple river water filtration (Figure 6(b)). Interestingly, the PA membrane remained unaltered after three hours of HONF as confirmed by membrane characterization via ATR-FTIR (Figure 9). It indicates that apparently no ozone residuals and radicals diffuse to the membrane surface. It likely

results from the fast ozone decomposition reactions with H_2O_2 and with some moieties of the NOM allowing to shorten the ozone lifetime in solution.

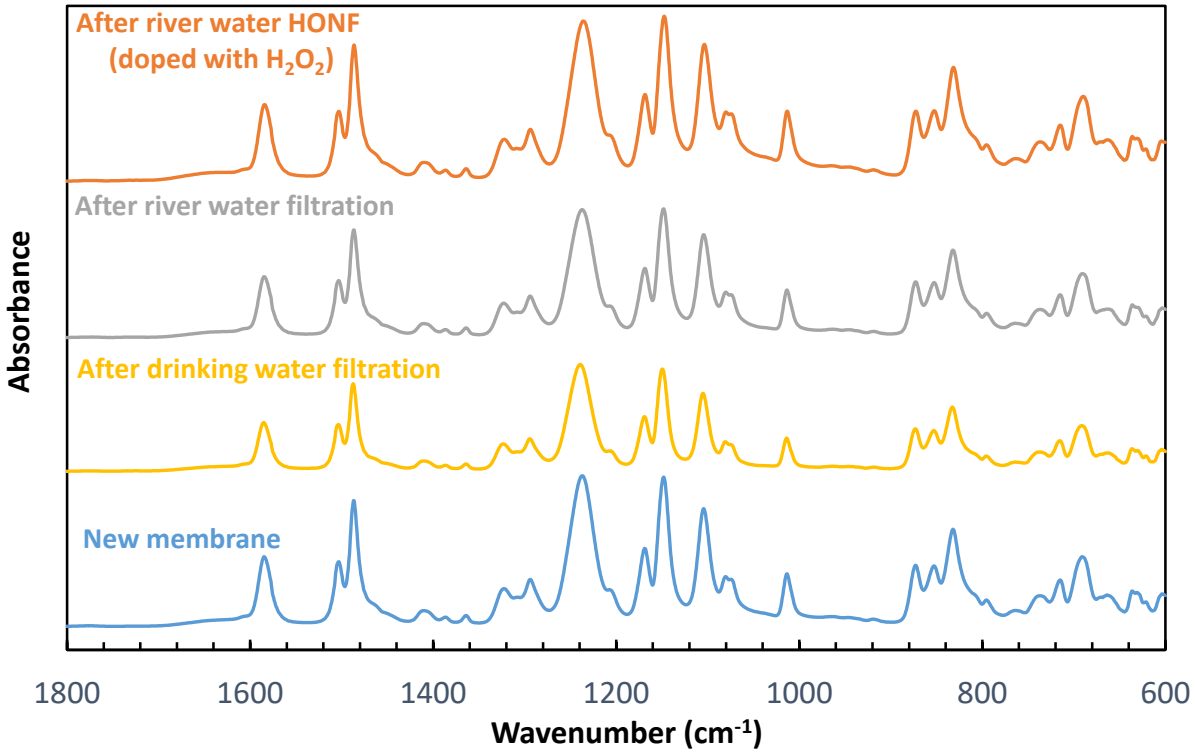

Figure 9: ATR-FTIR spectra of new and exposed NF270 PA membranes.

5. Conclusion

A monophasic hybrid ozone/nanofiltration process was developed, in which a pre-ozonated solution was mixed to the water to be treated before entrance in the membrane cell (Fig. 2(c)). Two organic membranes (NP10 PES and NF270 PA membranes) were considered despite a low ozone compatibility [30]. Without H_2O_2 doping, the ozone decomposition rate was too slow in the liquid bulk, leading to a significant dissolved ozone exposure ($\int C_{oz} dt$) concomitant with a fast membrane degradation observed in a few tens of minutes. Thus, addition of H_2O_2 (at equimolar concentration with respect to ozone) was advantageous to enhance the ozone decomposition rate in the liquid bulk and to lower the ozone exposure, allowing to protect the membrane.

During the HONF of the drinking water doped with H_2O_2, overall ozone and DEA removal yields of around 91% and 54%, respectively, were measured with the NP10 PES membrane, without significant solute concentration owing to the fact that this membrane has a high MWCO (1000-1200 Da). The observed DEA removal yield was correlated to a very high radical generation rate, characterized by R_{ct} at the orders of magnitude of 10^{-6}. Besides, in that case, two pharmaceuticals (CBZ and SMX), having high reactivity with molecular ozone, were efficiently removed in both the permeate and the retentate, with concentrations lower than the detection limits.

During the filtration of a river water sample, characterized by a high DOC around 10 ppm, the ozone decomposition rate was enhanced owing to the fact that some moieties of the natural organic matter can initiate the ozone decomposition [32,42,60]. Consequently, no degradation of both the NF270 PA and PES membrane surfaces was noticed, even if the PA membrane is particularly sensitive to ozone [30]. It confirms that H_2O_2 and the NOM concentrated at the membrane surface can have as screening effect, avoiding ozone diffusion to the membrane surface. Nonetheless, the radical generation exposure decreased by around a factor 10 compared to drinking water, showing that NOM might also play the role of radical scavengers. Furthermore, the membrane fouling was decreased by a factor two after one hour of operation compared to filtration without hybrid ozonation (Fig. 2(a)). With the tighter NF270 PA membrane (200-300 Da), a synergy between the oxidation and rejection was observed. DOC and DEA removal efficiencies up to 70% in the permeate were therefore measured. A key point using ozone oxidation is the bromate formation. Nonetheless, intensive processes in which the ozone lifetime is reduced such as the one developed in this study should allow to limit bromate formation compared to traditional ozonation processes [4]. Further study will be nonetheless required to confirm it.

This prospective study shows that it would be possible to apply HONF in a monophasic configuration with commercial organic membranes providing that H_2O_2 is added to the water to be treated, especially using water with significant DOC content (for example some industrial waste waters or

considering reuse applications), which will exhibit a high ozone decomposition rate. This combination would improve the compactness of a water treatment chain (process intensification) in order to mitigate the membrane fouling and to increase the ozone decomposition and radicals generation rates, especially with tight membranes which can concentrate H_2O_2 and the NOM involved during the ozone decomposition initiation. Compared to the gas-liquid HONF configuration [6,18], in which ozone is dissolved in water directly in the membrane module, the monophasic configuration presented in this study has several benefits, (i) an easier implementation and an easier control of the oxidants dosage, since the ozone dissolution can be carried out independently of the membrane filtration stage; (ii) a high potential to generate *in-situ* radicals owing to the fast ozone decomposition initiated by H_2O_2 and NOM [42]; (iii) a low ozone exposure in the liquid bulk allowing to limit (or suppress) the dissolved ozone diffusion at the membrane surface; and (iv) the absence of an ozone-enriched gas-phase, allowing to consider organic membranes instead of more expensive ceramic membranes.

To validate the potential of this hybrid process, a pilot study performed with a real waste water and a tight NF or LPRO membrane should be now implemented, especially to confirm (i), the robustness of the process after a long-term operating period and, (ii), the mitigation of the DOC content and of the micropollutant and their OTPs concentrations in the permeate. Higher permeate recovery rate (*RR*) should be targeted to lower the process water consumption and to increase the NOM concentration in the retentate to reinforce the screening effect that protects the membrane to the exposure to oxidants.

6. Acknowledgments

The Ministry of Higher Education and Scientific Research of Algeria and Campus France are gratefully acknowledged for providing S. Ouali with a Profas B+ grant (954610C). The Rennes 1 university is also acknowledged for providing PF Biard with a “Défi scientifique” grant. The authors are grateful to Nina Ramos, Pierre Largillière, Thierry Pain, Isabelle Soutrel, Valérie Couroussé and Christelle Gardin for technical assistance.

References list

[1] P.E. Stackelberg, J. Gibs, E.T. Furlong, M.T. Meyer, S.D. Zaugg, R.L. Lippincott, Efficiency of conventional drinking-water-treatment processes in removal of pharmaceuticals and other organic compounds, Sci. Total Environ. 377 (2007) 255–272. https://doi.org/10.1016/j.scitotenv.2007.01.095.

[2] O.M. Rodriguez-Narvaez, J.M. Peralta-Hernandez, A. Goonetilleke, E.R. Bandala, Treatment technologies for emerging contaminants in water: A review, Chem. Eng. J. 323 (2017) 361–380.

[3] S.P. Dharupaneedi, S.K. Nataraj, M. Nadagouda, K.R. Reddy, S.S. Shukla, T.M. Aminabhavi, Membrane-based separation of potential emerging pollutants, Sep. Purif. Technol. 210 (2019) 850–866.

[4] U. von Gunten, Oxidation processes in water treatment: are we on track?, Environ. Sci. Technol. 52 (2018) 5062–5075.

[5] C. Bellona, J.E. Drewes, P. Xu, G. Amy, Factors affecting the rejection of organic solutes during NF/RO treatment—a literature review, Water Res. 38 (2004) 2795–2809.

[6] S.O. Ganiyu, E.D. van Hullebusch, M. Cretin, G. Esposito, M.A. Oturan, Coupling of membrane filtration and advanced oxidation processes for removal of pharmaceutical residues: A critical review, Sep. Purif. Technol. 156 (2015) 891–914. https://doi.org/10.1016/j.seppur.2015.09.059.

[7] S. Kim, K.H. Chu, Y.A.J. Al-Hamadani, C.M. Park, M. Jang, D.-H. Kim, M. Yu, J. Heo, Y. Yoon, Removal of contaminants of emerging concern by membranes in water and wastewater: A review, Chem. Eng. J. 335 (2018) 896–914. https://doi.org/10.1016/j.cej.2017.11.044.

[8] J.L. Acero, F.J. Benitez, F. Teva, A.I. Leal, Retention of emerging micropollutants from UP water and a municipal secondary effluent by ultrafiltration and nanofiltration, Chem. Eng. J. 163 (2010) 264–272. https://doi.org/10.1016/j.cej.2010.07.060.

[9] Y. Liu, X. Wang, H. Yang, Y.F. Xie, Quantifying the influence of solute-membrane interactions on adsorption and rejection of pharmaceuticals by NF/RO membranes, J. Membr. Sci. 551 (2018) 37–46. https://doi.org/10.1016/j.memsci.2018.01.035.

[10] Y. Yoon, P. Westerhoff, S.A. Snyder, E.C. Wert, J. Yoon, Removal of endocrine disrupting compounds and pharmaceuticals by nanofiltration and ultrafiltration membranes, Desalination. 202 (2007) 16–23. https://doi.org/10.1016/j.desal.2005.12.033.

[11] M.A. Oturan, J.-J. Aaron, Advanced oxidation processes in water/wastewater treatment: principles and applications. A review, Crit. Rev. Environ. Sci. Technol. 44 (2014) 2577–2641.

[12] J.L. Acero, U. Von Gunten, Characterization of oxidation processes : ozonation and the AOP O_3/H_2O_2, J. Am. Water Works Assoc. 93 (2001) 90–100.

[13] F.J. Beltrán, Theoretical aspects of the kinetics of competitive first reactions of ozone in the O_3/H_2O_2 and O_3/UV oxidation processes, Ozone Sci. Eng. 19 (1997) 13–38.

[14] E.J. Rosenfeldt, K.G. Linden, S. Canonica, U. von Gunten, Comparison of the efficiency of OH radical formation during ozonation and the advanced oxidation processes O_3/H_2O_2 and UV/H_2O_2, Water Res. 40 (2006) 3695–3704. http://dx.doi.org/10.1016/j.watres.2006.09.008.

[15] J. Staehelin, J. Hoigne, Decomposition of ozone in water: rate of initiation by hydroxide ions and hydrogen peroxide, Environ. Sci. Technol. 16 (1982) 676–681.

[16] U. Von Gunten, Ozonation of drinking water: Part I. Oxidation kinetics and product formation, Water Res. 37 (2003) 1443–1467.

[17] M. Bourgin, E. Borowska, J. Helbing, J. Hollender, H.-P. Kaiser, C. Kienle, C.S. McArdell, E. Simon, U. von Gunten, Effect of operational and water quality parameters on conventional ozonation and the advanced oxidation process O3/H2O2: Kinetics of micropollutant abatement, transformation product and bromate formation in a surface water, Water Res. 122 (2017) 234–245. https://doi.org/10.1016/j.watres.2017.05.018.

[18] C. Mansas, J. Mendret, S. Brosillon, A. Ayral, Coupling catalytic ozonation and membrane separation: A review, Sep. Purif. Technol. 236 (2020) 116221. https://doi.org/10.1016/j.seppur.2019.116221.

[19] S. Byun, J.S. Taurozzi, V.V. Tarabara, Ozonation as a pretreatment for nanofiltration: Effect of oxidation pathway on the permeate flux, Sep. Purif. Technol. 149 (2015) 174–182. https://doi.org/10.1016/j.seppur.2015.05.035.

[20] L. Flyborg, B. Björlenius, K.M. Persson, Can treated municipal wastewater be reused after ozonation and nanofiltration? Results from a pilot study of pharmaceutical removal in Henriksdal WWTP, Sweden, Water Sci. Technol. 61 (2010) 1113–1120. https://doi.org/10.2166/wst.2010.029.

[21] B.S. Oh, H.Y. Jang, T.M. Hwang, J.-W. Kang, Role of ozone for reducing fouling due to pharmaceuticals in MF (microfiltration) process, J. Membr. Sci. 289 (2007) 178–186.

[22] H. Vatankhah, C.C. Murray, J.W. Brannum, J. Vanneste, C. Bellona, Effect of pre-ozonation on nanofiltration membrane fouling during water reuse applications, Sep. Purif. Technol. 205 (2018) 203–211. https://doi.org/10.1016/j.seppur.2018.03.052.

[23] J.L. Acero, F.J. Benitez, F.J. Real, E. Rodriguez, Elimination of selected emerging contaminants by the combination of membrane filtration and chemical oxidation processes, Water. Air. Soil Pollut. 226 (2015) 1–14.

[24] G.R. Pophali, S. Hedau, N. Gedam, N.N. Rao, T. Nandy, Treatment of refractory organics from membrane rejects using ozonation, J. Hazard. Mater. 189 (2011) 273–277.

[25] A.L. Alpatova, S.H. Davies, S.J. Masten, Hybrid ozonation-ceramic membrane filtration of surface waters: The effect of water characteristics on permeate flux and the removal of DBP precursors, dicloxacillin and ceftazidime, Sep. Purif. Technol. 107 (2013) 179–186. https://doi.org/10.1016/j.seppur.2013.01.013.

[26] S. Byun, S.H. Davies, A.L. Alpatova, L.M. Corneal, M.J. Baumann, V.V. Tarabara, S.J. Masten, Mn oxide coated catalytic membranes for a hybrid ozonation–membrane filtration: Comparison

of Ti, Fe and Mn oxide coated membranes for water quality, Water Res. 45 (2011) 163–170. https://doi.org/10.1016/j.watres.2010.08.031.

[27] J. Kim, S.H.R. Davies, M.J. Baumann, V.V. Tarabara, S.J. Masten, Effect of ozone dosage and hydrodynamic conditions on the permeate flux in a hybrid ozonation–ceramic ultrafiltration system treating natural waters, J. Membr. Sci. 311 (2008) 165–172. https://doi.org/10.1016/j.memsci.2007.12.010.

[28] N. Rosman, W.N.W. Salleh, M.A. Mohamed, J. Jaafar, A.F. Ismail, Z. Harun, Hybrid membrane filtration-advanced oxidation processes for removal of pharmaceutical residue, J. Colloid Interface Sci. 532 (2018) 236–260.

[29] T. Coward, H. Tribe, A.P. Harvey, Opportunities for process intensification in the UK water industry: A review, J. Water Process Eng. 21 (2018) 116–126. https://doi.org/10.1016/j.jwpe.2017.11.010.

[30] S. Ouali, P. Loulergue, P.-F. Biard, N. Nasrallah, A. Szymczyk, Ozone compatibility with polymer nanofiltration membranes, J. Membr. Sci. 618 (2021) 118656. https://doi.org/10.1016/j.memsci.2020.118656.

[31] Y. Mori, T. Oota, M. Hashino, M. Takamura, Y. Fujii, Ozone-microfiltration system, Desalination. 117 (1998) 211–218.

[32] M.O. Buffle, U. Von Gunten, Phenols and amine induced HO° generation during the initial phase of natural water ozonation, Environ. Sci. Technol. 40 (2006) 3057–3063.

[33] M.S. Elovitz, U. Von Gunten, Hydroxyl radical/ozone ratios during ozonation processes. I. The R_{ct} concept, Ozone Sci. Eng. 21 (1999) 239–260.

[34] J. Yang, J. Li, W. Dong, J. Ma, T. Li, Y. Yang, J. Li, J. Gu, Deethylatrazine as a more appropriate hydroxyl radical probe compound during ozonation: comparison with the widely used p-chlorobenzoic acid, Chem. Eng. J. 295 (2016) 443–450.

[35] R. Gulde, B. Clerc, M. Rutsch, J. Helbing, E. Salhi, C.S. McArdell, U. von Gunten, Oxidation of 51 micropollutants during drinking water ozonation: Formation of transformation products and

their fate during biological post-filtration, Water Res. 207 (2021) 117812. https://doi.org/10.1016/j.watres.2021.117812.

[36] M.N. Abellán, W. Gebhardt, H.Fr. Schröder, Detection and identification of degradation products of sulfamethoxazole by means of LC/MS and −MSn after ozone treatment, Water Sci. Technol. 58 (2008) 1803–1812. https://doi.org/10.2166/wst.2008.539.

[37] M. del M. Gómez-Ramos, M. Mezcua, A. Agüera, A.R. Fernández-Alba, S. Gonzalo, A. Rodríguez, R. Rosal, Chemical and toxicological evolution of the antibiotic sulfamethoxazole under ozone treatment in water solution, J. Hazard. Mater. 192 (2011) 18–25. https://doi.org/10.1016/j.jhazmat.2011.04.072.

[38] U. Hübner, B. Seiwert, T. Reemtsma, M. Jekel, Ozonation products of carbamazepine and their removal from secondary effluents by soil aquifer treatment – Indications from column experiments, Water Res. 49 (2014) 34–43. https://doi.org/10.1016/j.watres.2013.11.016.

[39] U. Hübner, U. von Gunten, M. Jekel, Evaluation of the persistence of transformation products from ozonation of trace organic compounds – A critical review, Water Res. 68 (2015) 150–170. https://doi.org/10.1016/j.watres.2014.09.051.

[40] T.T. Dang, P.-F. Biard, A. Couvert, Assessment of a Stirred-Cell Reactor Operated Semicontinuously for the Kinetic Study of Fast Direct Ozonation Reactions by Reactive Absorption, Ind. Eng. Chem. Res. 55 (2016) 8058–8069. https://doi.org/10.1021/acs.iecr.6b02025.

[41] C.F. Couto, A.V. Santos, M.C.S. Amaral, L.C. Lange, L.H. de Andrade, A.F.S. Foureaux, B.S. Fernandes, Assessing potential of nanofiltration, reverse osmosis and membrane distillation drinking water treatment for pharmaceutically active compounds (PhACs) removal, J. Water Process Eng. 33 (2020) 101029.

[42] P.-F. Biard, T.T. Dang, J. Bocanegra, A. Couvert, Intensification of the O_3/H_2O_2 advanced oxidation process using a continuous tubular reactor filled with static mixers: Proof of concept, Chem. Eng. J. 344 (2018) 574–582. https://doi.org/10.1016/j.cej.2018.03.112.

[43] P.-F. Biard, T.T. Dang, A. Couvert, Determination by reactive absorption of the rate constant of the ozone reaction with the hydroperoxide anion, Chem. Eng. Res. Des. 127 (2017) 62–71.

[44] M.G. Evans, N. Uri, The dissociation constant of hydrogen peroxide and the electron affinity of the HO 2 radical, Trans. Faraday Soc. 45 (1949) 224–230.

[45] R. Loos, R. Niessner, Analysis of atrazine, terbutylazine and their N-dealkylated chloro and hydroxy metabolites by solid-phase extraction and gas chromatography–mass spectrometry and capillary electrophoresis–ultraviolet detection, J. Chromatogr. A. 835 (1999) 217–229.

[46] D.C. McDowell, M.M. Huber, M. Wagner, U. von Gunten, T.A. Ternes, Ozonation of Carbamazepine in Drinking Water: Identification and Kinetic Study of Major Oxidation Products, Environ. Sci. Technol. 39 (2005) 8014–8022. https://doi.org/10.1021/es050043l.

[47] T. Scheytt, P. Mersmann, R. Lindstädt, T. Heberer, 1-Octanol/water partition coefficients of 5 pharmaceuticals from human medical care: carbamazepine, clofibric acid, diclofenac, ibuprofen, and propyphenazone, Water. Air. Soil Pollut. 165 (2005) 3–11.

[48] A.L. Boreen, W.A. Arnold, K. McNeill, Photochemical Fate of Sulfa Drugs in the Aquatic Environment: Sulfa Drugs Containing Five-Membered Heterocyclic Groups, Environ. Sci. Technol. 38 (2004) 3933–3940. https://doi.org/10.1021/es0353053.

[49] Y. Huang, J. Guo, P. Yan, H. Gong, F. Fang, Sorption-desorption behavior of sulfamethoxazole, carbamazepine, bisphenol A and 17α-ethinylestradiol in sewage sludge, J. Hazard. Mater. 368 (2019) 739–745.

[50] M.M. Huber, S. Canonica, G.-Y. Park, U. von Gunten, Oxidation of Pharmaceuticals during Ozonation and Advanced Oxidation Processes, Environ. Sci. Technol. 37 (2003) 1016–1024. https://doi.org/10.1021/es025896h.

[51] C.-L. Zhang, F.-A. Wang, Y. Wang, Solubilities of sulfadiazine, sulfamethazine, sulfadimethoxine, sulfamethoxydiazine, sulfamonomethoxine, sulfamethoxazole, and sulfachloropyrazine in water from (298.15 to 333.15) K, J. Chem. Eng. Data. 52 (2007) 1563–1566.

[52] B.K. Bezbarua, D.A. Reckhow, Modification of the standard neutral ozone decomposition model, Ozone Sci. Eng. 26 (2004) 345–357.

[53] J. Staehelin, R.E. Buehler, J. Hoigne, Ozone decomposition in water studied by pulse radiolysis. 2. Hydroxyl and hydrogen tetroxide (HO_4°) as chain intermediates, J. Phys. Chem. 88 (1984) 5999–6004.

[54] J. Rodier, L'analyse de l'eau, 8ème édition, Paris, 1996.

[55] H. Bader, J. Hoigne, Determination of ozone in water by the Indigo method, Water Res. 15 (1981) 1573–1580.

[56] K. Li, S. Li, Q. Su, G. Wen, T. Huang, Effects of hydrogen peroxide and sodium hypochlorite aging on properties and performance of polyethersulfone ultrafiltration membrane, Int. J. Environ. Res. Public. Health. 16 (2019) 3972.

[57] M.T. Tsehaye, J. Wang, J. Zhu, S. Velizarov, B. Van der Bruggen, Development and characterization of polyethersulfone-based nanofiltration membrane with stability to hydrogen peroxide, J. Membr. Sci. 550 (2018) 462–469. https://doi.org/10.1016/j.memsci.2018.01.022.

[58] Y. Hanafi, P. Loulergue, S. Ababou-Girard, C. Meriadec, M. Rabiller-Baudry, K. Baddari, A. Szymczyk, Electrokinetic analysis of PES/PVP membranes aged by sodium hypochlorite solutions at different pH, J. Membr. Sci. 501 (2016) 24–32. https://doi.org/10.1016/j.memsci.2015.11.041.

[59] Y. Kourde-Hanafi, P. Loulergue, A. Szymczyk, B. Van der Bruggen, M. Nachtnebel, M. Rabiller-Baudry, J.-L. Audic, P. Pölt, K. Baddari, Influence of PVP content on degradation of PES/PVP membranes: Insights from characterization of membranes with controlled composition, J. Membr. Sci. 533 (2017) 261–269. https://doi.org/10.1016/j.memsci.2017.03.050.

[60] M.-O. Buffle, J. Schumacher, E. Salhi, M. Jekel, U. Von Gunten, Measurement of the initial phase of ozone decomposition in water and wastewater by means of a continuous quench-

flow system: Application to disinfection and pharmaceutical oxidation, Water Res. 40 (2006) 1884–1894.

[61] M.S. Elovitz, U. Von Gunten, H.P. Kaiser, Hydroxyl radical/ozone ratios during ozonation processes. II. The effect of temperature, pH, alkalinity, and DOM properties, Ozone Sci. Eng. 22 (2000) 123–150.

[62] E.L. Yong, Y.-P. Lin, Incorporation of initiation, promotion and inhibition in the R_{ct} concept and its application in determining the initiation and inhibition capacities of natural water in ozonation, Water Res. 46 (2012) 1990–1998.

[63] G.V. Buxton, C.L. Greenstock, W.P. Helman, A.B. Ross, W. Tsang, Critical review of rate constants for reactions of hydrated electrons, hydrogen atoms and hydroxyl radicals ($OH^{\bullet}/O^{\bullet-}$) in aqueous solution, J. Phys. Chem. Ref. Data. 17 (1988) 513–886.